References

[1] K. Osozawa and N. Okato, Passivity and its Breakdown on Iron and Iron Based Alloys. (USA-Japan Seminar, Honolulu), Houston, TX NACE (1976) 135.

[2] R. Bandy and D. Van Rooyen, Corros. 39 (1983) 227.

[3] Y. C. Lu, R. Bandy C. R. Clayton and R. C. Newman, J. Electrochem. Soc. 130 (1983) 1774.

[4] J. E. Truman, M. J. Coleman and K. R. Prit. Corros. J. 12 (1977) 236.

[5] J. Eckenrod and C. W, Kovack, ASTM STP 679, p17 Philadelphia, PA (1977).

[6] L. Wegrelius and I. Olefjord, Proceedings of the 12 th International Corrosion Congress, Houston, Texas, USA, NACE International, Vol. 5B (1993) 3886.

[7] A. Sadough-Vanini, J.P. Audourad and P. Marcus, Corrosion Science, 36 (1994) 1825.

[8] A. Sadough-Vanini, R. Chikhi and P. Marcus, Proceedings of UK Corrosion 94 and Eurocorr 94 .

[9] I. Olefjord, Mat. Science and Engineering, 42 (1980) 161.

[10] I. Olefjord, B. Brox and U. Jelvestam, J. Electrochem. Soc. 132 (1985) 2854.

[11] C. R. Clayton and Y. C. Lu, J. Electrochemical . Soc., 133 (1986) 2465.

[12] J. E. Castle and J. H. Qiu, Corrosion Science, 30 (1990) 429.

[13] C. R. Clayton, L.Rosensweig, M. Oversluizen and Y. C. Lu, in: Surfaces , Inhibition and Passivation, Eds. E. Mc-Cafferty and R. J. Brod (The Electrochemical Society, Pennington, NJ) (1986) 323.

[14] I. Olefjord and C. R. Clayton, in Corrosion Mechanisms in Theory and Practice, Eds. P. Marcus and J. Oudar, Marcel Dekker (NY) (1995) p. 175.

[15] E. De Vito and P. Marcus Surface Interface Analysis, 19 (1992) 403.

[16] E. DE Vito and P. Marcus, Proceedings of the 12th International Corrosion Congress, Houston, Texas, USA, NACE International, Vol. 5B (1993) 3898.

[17] P. Marcus and M. E. Bussell, Appl. Surf. Sci. 59 (1992) 7.

[18] Y. Arnaud and M. Brunel Appl. Surf.Sci. 35 (1989) 345.

[19] L. Beaunier, Private communication.

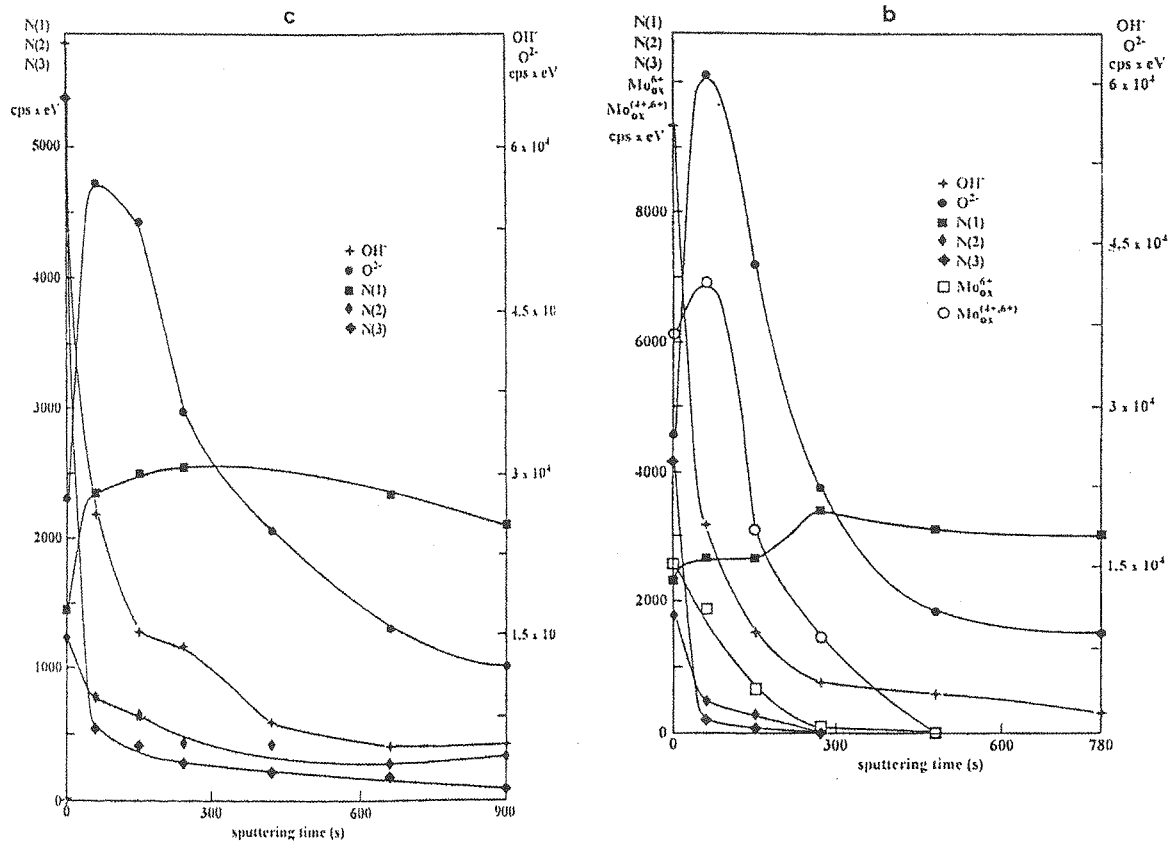

Fig (6) XPS depth profiles of passivated Mo-N implanted alloy:, (b) (R2) and (c) (R3)

Table (1) Chemical analysis of the austenitic stainless steel before implantation

Element	Fe	Cr	Ni	Mn	Si	Cu	Mo	C	N	P	S
Concentration (wt %)	72.01	17.38	8.28	1.43	0.49	0.15	0.14	0.05	0.04	0.03	0.0025

Table (2) Ion implantation conditions

Implanted ion	Dose	Energy	Residual pressure during implantation	Temperature
Mo^+	2.5 10^{16}at.cm^{-2}	100 Kev	10^{-5} torr	Room temp.
N_2^+	2.5 10^{16}at.cm^{-2}	100 Kev	10^{-5} torr	Room temp.

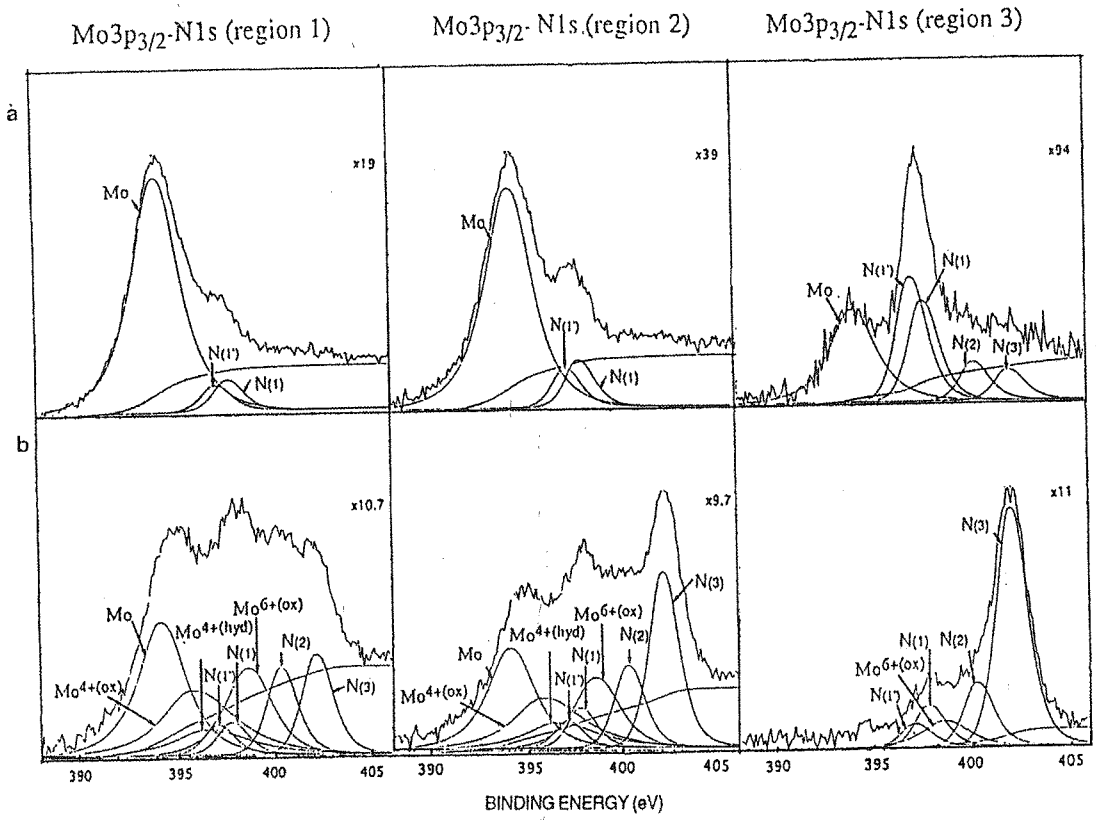

Fig (5) XPS spectra of Mo3p-N1s corresponding to the first (R1), second (R2) and third (R3) regions (a) before passivation and (b) after passivation.

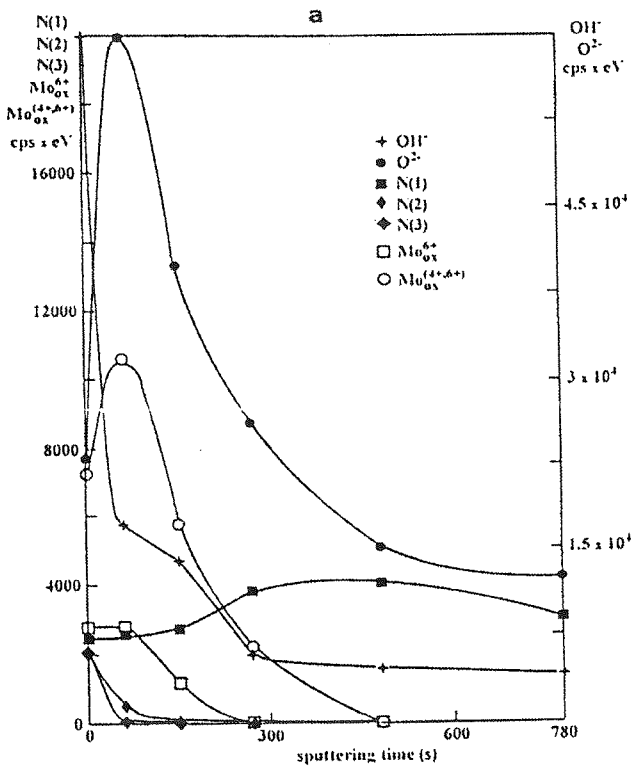

Fig (6) XPS depth profiles of passivated Mo-N implanted alloy: (a) (R1)

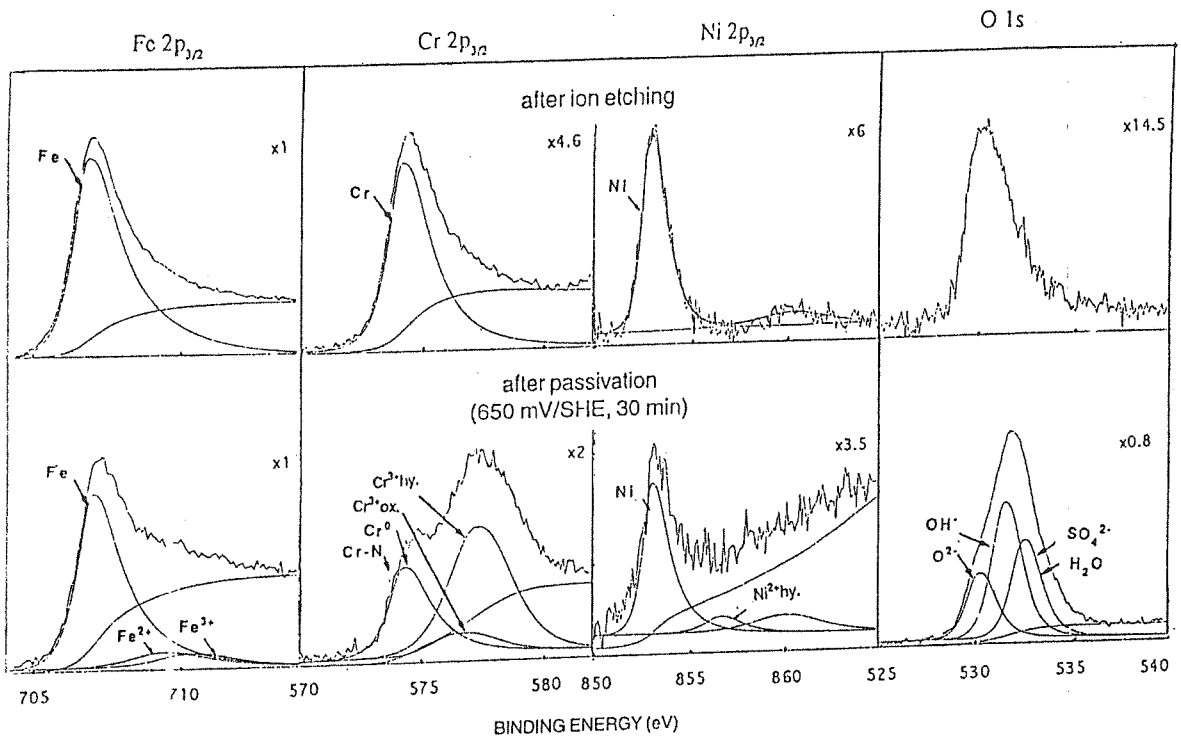

Fig. (3) XPS spectra of Fe2p3/2, Cr2p3/2, Ni2p3/2 and O1s, for the implanted alloy (first region in the depth profiles, R1) (a) before passivation, (b) after passivation.

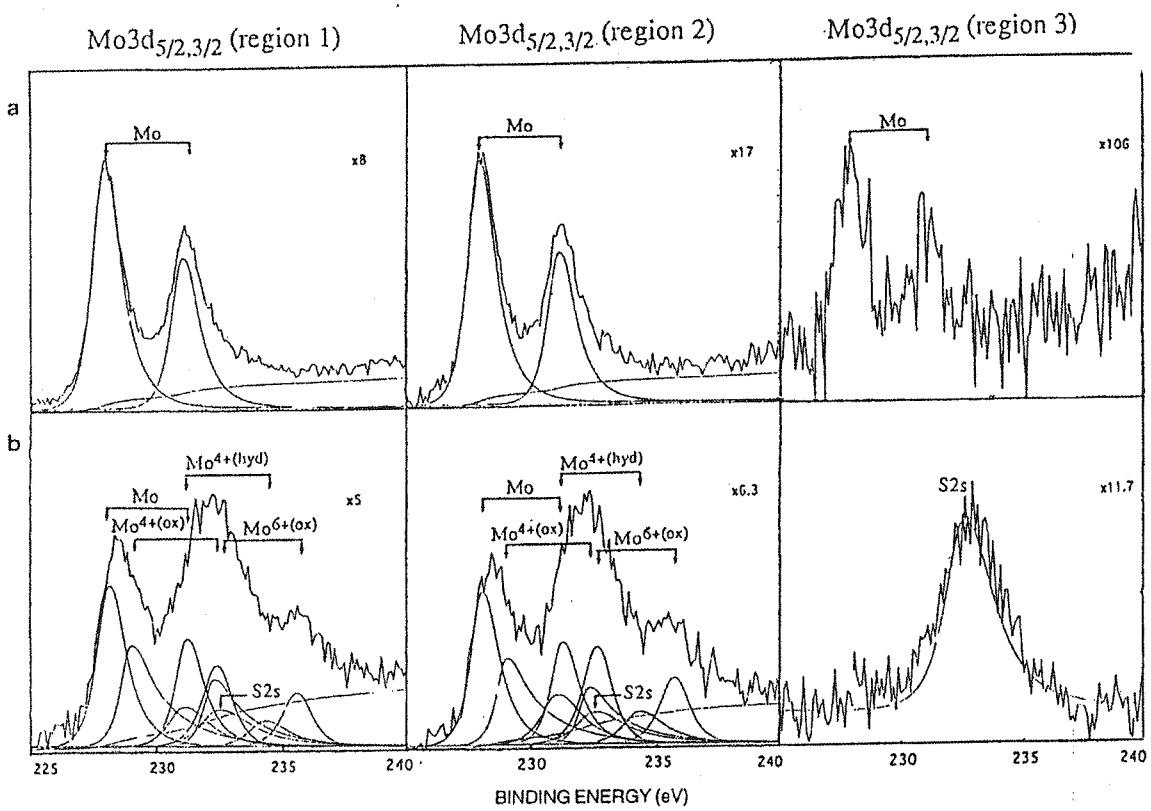

Fig (4) XPS spectra of Mo3d corresponding to the first (R1), second (R2) and third (R3) regions (a) before passivation and (b) after passivation.

active state is found to be markedly moderated by Mo and slightly enhanced by nitrogen. For the high concentration of Mo the activation peak disappears, and the residual current density is higher in the 100-500 mV/SHE potential region, where an oxidation or dissolution process occurs.

The passive film consists of an inner barrier oxide film and an outer hydroxide film. The hydroxide layer present on the surface of the passive films is enriched with Mo^{6+}. Mo^{4+} is also found in the passive film. Nitrogen is found in three chemical states. The low binding energy N1s originates from the implanted nitrogen segregated at the alloy-passive film interface.

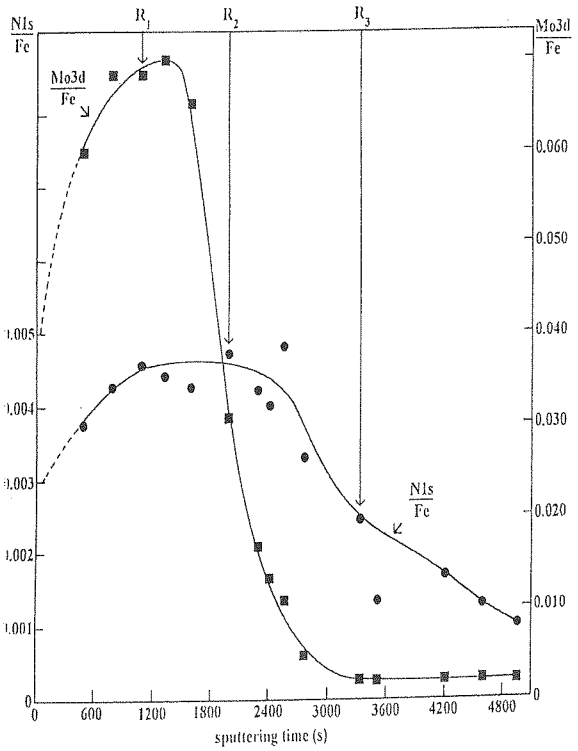

Fig. (1) XPS sputtering depth profiles of Mo and N in the co-implanted austenitic stainless steel.

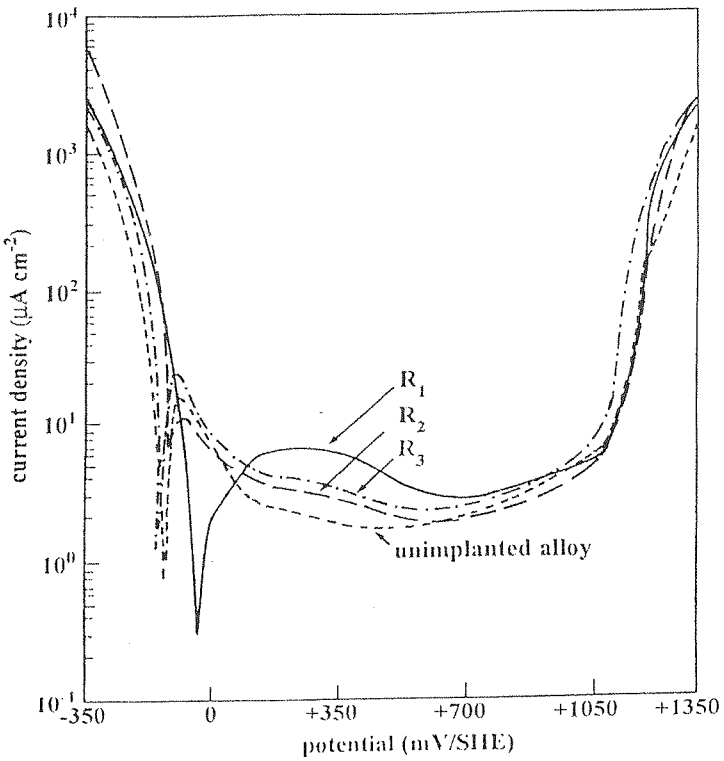

Fig (2) Potentiodynamic curves of the non-implanted alloy and of the Mo-N implanted alloy for the three surface concentrations R1, R2 and R3 (0. 5 M H2 SO4, 1mV/sec) - R1 (7at% Mo and 2.7at%N) - R2 (2. 80t% Mo and 2.8 at%N - R3 (0.3at% Mo and 1.6at%N) - 304type stainless steel.

(OH^-) forms. A third peak is present at higher binding energy corresponding to oxygen in H_2O and SO_4^{2-}. Oxidized molybdenum is detected in the analysed passive film formed on the Mo-N implanted alloy surfaces. The Mo3d regions have been resolved by curve fitting (Fig.4) into the metallic form of Mo implanted in the alloy (277.8 and 231 eV) and three oxide states: Mo^{4+ox} (229.1 and 232.3), Mo^{4+hyd} (231.1 and 234.3eV) and Mo^{6+ox} (232.5 and 235.7eV). The curve fitting of the Mo3d spectra shows that Mo is mainly present in the passive film in the form of Mo^{4+} and Mo^{+6} . The XPS spectra of the Mo3p-N1s region after passivation for the three surface concentrations (R1, R2, and R3) were fitted by 8 peaks corresponding to 4 Mo chemical states and 4 N chemical states (Fig.5). The peaks used for Mo are the following:Mo^{met} (394eV), Mo^{4+ox} (395.7eV), Mo^{4+hyd} (396.4eV) and Mo^{6+ox} (398.5eV). The N1s signal emitted by nitrogen implanted in the alloy was fitted by two peaks: one at 397.7eV, similar to the signal revealed on high nitrogen stainless steels (8), and an additional peak located at 397eV which was found necessary to obtain a good fit of the experimental spectrum and which may be due to ion implantation. Two nitrogen peaks N (2) and N (3) located at higher binding energies (400.2 and 402 eV) may originate from N-H (NH_3, NH_4^+) or N-O species (13, 17). The relative intensity of the low binding energy (N1s) signals N (1) is higher after passivation, showing the enrichment of nitrogen.

Argon ion sputtering depth profiles have been recorded and are shown in Fig. 6 (a, b and c) for the three initial surface concentrations of Mo and N (R1, R2 and R3). The profiles of OH^- and O^{2-} are indicative of the bilayer structure of the film (inner oxide and outer hydroxide). The decrease of the Mo^{6+} signal observed after the first ion sputtering indicates that Mo^{6+} is located in the outer part of the passive film, as are the high binding energy nitrogen species (N (2) and N (3)). The sputtering depth profiles confirm the enrichment of nitrogen in the inner part of the film. Nitrogen segregates by anodic segregation during the dissolution stage preceding passivation and accumulates at the alloy/passive film interface where nitride islands can be formed, as shown previously for N-implanted stainless steels (17). The large amount of nitrid segregated on the surface during dissolution/ passivation of the (Mo-N) implanted alloy does not improve further the corrosion resistance and even appears to be somewhat detrimental, as dissolution in the active state was found to be enhanced by nitrogen when the Mo-contain of the alloy was low.

Conclusion

Molybdenum and nitrogen co-implanted austenitic stainless steels have been studied by electrochemical measurements and XPS analysis. The implantation profiles have been characterized by XPS. Prior to electrochemical experiments the co-implanted alloys were sputtered to obtain different concentrations of Mo and N. The effects of the implanted molybdenum and nitrogen on the electrochemical behaviour of the alloy in 0.5 M H_2SO_4 have been investigated. The surface films have been analysed by XPS.

As the concentration of Mo decreases and the nitrogen increases it is observed that the current in the active region of the polarization increases i.e dissolution in the

less steel. The concentration of N increases up to 3at% and then decreases to finally approach the N concentration of unimplanted 304-type stainless steel. It must be noted that a $\gamma \rightarrow \alpha$ phase transformation induced by the implantation of Mo has been observed by TEM (18, 19) on samples prepared under similar conditions. Knowing the implantation profiles of the samples, well-defined surface concentrations of Mo and N could be prepared by controlled argon ion-etching prior to the electrochemical measurements. The co-implanted alloys were sputtered for 22, 35 and 45 minutes, in order to produce surfaces with N and Mo concentrations corresponding approximately to 97% C_{Mo}^{max} - 94%C_N^{max} (first region, denoted R1 in Fig. 1), 40% C_{Mo}^{max} - 97%C_N^{max} (second region, denoted R2) and 4% C_{Mo}^{max}-53%C_N^{max} (third region, denoted R3). C_{Mo}^{max} and C_N^{max} are the Mo and N concentrations at the maximum in the profiles of Mo and N, respectively. Using the data reported above for C_{Mo}^{max} and C_N^{max} in separate implantation experiments, the corresponding concentrations are calculated to be 7at%Mo-2.7at%N, 2.8at%Mo-2.8at%N and 0.3at% Mo-1.6at%N for the R1,R2 and R3 regions, respectively.

Electrochemical behaviour of the co-implanted alloy

The i-E plots for the (Mo-N) implanted alloy with the initial surface concentrations corresponding to R1, R2 and R3 and for the unimplanted 304-type stainless steel are shown in Fig.2. The major effect is the decrease of the current in the active region for increasing Mo surface concentration. Nitrogen has a much less marked, non-beneficial effect. On the surface with the high concentration of Mo, the activation peak is suppressed. The current density is however higher in the 100-500 mV/SHE potential region, where an oxidation/dissolution process occurs (15). The high potential region of passivity is similar for the three concentrations of Mo and N and for the non-implanted alloy.

Surface analysis

For the XPS study of the passive films, the potential was stepped to 650 m V/SHE (which is in the passive region for all analysed samples) and the samples were polarized 30 min. The $Fe2p_{3/2}$, $Cr2p_{3/2}$, $Ni2p_{3/2}$ and O1s spectra obtained for the "Rl" region (high Mo-high N) before and after passivation are shown in Fig.3 and the Mo3d, Mo3p and Nls spectra are shown in Figs.4 and 5 for all three regions (Rl, R2 and R3) before and after passivation. Oxidized iron (Fe^{2+} and Fe^{3+}) is found in the passive film though in much smaller quantities than oxidized chromium. There is no significant signal from nickel oxide after passivation, in agreement with other works (7-12). The weak Ni^{met} signal observed in the $Ni2p_{3/2}$ region is emitted by Ni in the alloy. In the $Cr2p_{3/2}$ spectrum, a broad intense peak at low binding energy (574.3 eV) is assigned to chromium in the underlying alloy and chromium located in the film and bonded to nitrogen (17). The chromium $Cr2p_{3/2}$ region was resolved by curve fitting into the metallic Cr and Cr-N states mentioned above (572.3eV), chromium oxide denoted Cr^{3tox} (576.6 eV) and chromium hydroxide denoted Cr^{3+hyd} (577.2 eV). The results indicate a marked enrichment in Cr^{3+} in the passive film. The oxygen signal clearly reveals the presence of the oxide (O^{2-}) and hydroxide

work was to investigate the behaviour of alloys implanted with both Mo and N, which provide the possibility to vary the initial surface concentrations of both elements.

Experimental Procedure

The austenitic stainless steel (Fe17Cr8Ni (wt%)) used in this research was provided by UGINE (France). The alloy composition is given in Table 1. The samples were implanted first with Mo and then with N ions at NITRUVIDE (France). The implantation conditions are reported in Table 2. Sample discs of 10 mm diameter were cut from the implanted steels by spark erosion, following which they were cleaned ultrasonically with acetone and rinsed in ethanol and pure water. XPS studies have been performed with a VG ESCALAB Mark II spectometer using the Al Kα X-ray source (hν = 1486.6 eV) and a hemispherical analyser with a pass energy of 20 eV for the high resolution spectra. The reference for the reported binding energies are $Au4f_{7/2}$ at 83.8 eV and $Cu2p_{3/2}$ at 932.7 eV. Composition depth profiles were obtained by sputtering the surface with argon ions. Two ion guns were used , a VG AG21 ion gun, mounted in the preparation chamber attached to the spectrometer, for the preparation of the samples prior to passivation (ion beam acceleration voltage 2kV, argon pressure $pAr=7\times10^{-6}$ mbar, and ion beam current density 100μ A/cm^2), and a VG AG60 ion gun with differential pumping, mounted in the analysis chamber, used for sputter depth profiling of the passive films (4 KV, 0.5μA/cm^2). After preparation of the surface by ion sputtering, the sample was transferred in a transfer vessel under pure nitrogen into a nitrogen-filled glove box where the electrochemical experiments were carried out. The electrochemical cell was composed of a saturated sulfate reference electrode, a platinum counter electrode and the working electrode. A PAR 273 potentiostat interfaced to a computer was used. The electrolyte was 0.5 M H_2SO_4 prepared with ultra-pure water and pure sulphuric acid. After passivation, the samples were removed from the cell under applied potential, rinsed in ultra pure water, dried in nitrogen and then transferred back to the spectrometer without exposure to air. XPS measurements and sputter depth profiling were then carried out.

Results and Discussion

Characterization of the implantation profiles in the co-implanted alloy and preparation of surfaces with various Mo and N concentrations for electrochemical measurements.

The co-implanted (Mo, N)-stainless steel was characterized by XPS. The surface of the implanted alloy was first analysed. The high resolution spectra of $Fe2p_{3/2}$., $Cr2p_{3/2}$ and O1s show that a thin oxide film (50A) is present on the surface. This oxide film was removed by ion sputtering prior to all electrochemical measurements. The XPS sputtering depth profiles are shown in Fig. 1. The profiles are plotted as the XPS N1s and $Mo3d_{5/2}$ to $Fe2p_{3/2}$ peak area ratio versus sputtering time. Simulations of the concentration profiles for the implantations of Mo and N have been performed in previous works (15-17). The maximum in the profile occurs at a depth below the surface of 150A for Mo and 580A for N. The concentration of Mo increases up to 8 at% and then decreases to finally approach the Mo concentration of the unimplanted 304-type stain-

Chemical Composition, Chemical States and Resistance to Localized Corrosion of Passive Films on the Nitrogen and Molybdenum Implanted Austenitic Stainless Steels

A. Sadough Vanini
Associate Professor
Mech. Engineering Department,
Amirkabir University of Technology

Abstract

XPS analysis and electrochemical measurements have been used to investigate the influence of Mo and N implantation on dissolution and passivation of 304 type stainless steel. The samples were implanted first with 100 Kev Mo^+ ions (2.5×10^{16} Mo at. cm^{-2}) and then with 100 KeV N_2^+ ions (2.5×10^{16} N at. cm^{-2}). Prior to the electrochemical experiments, surfaces with well-defined Mo and N concentrations were produced by argon ion sputtering the implanted alloy for a fixed time in the preparation chamber of the spectrometer in order to reach a well-defined point on the Mo and N depth profiles. Three regions of the implantation profiles with different Mo and N concentrations were investigated (high Mo-high N, medium Mo-high N and low Mo-medium N). The samples were transferred without air exposure from the spectrometer to an electrochemical cell mounted in a nitrogen-filled glove box.

The Mo-N co-implantation modifies the electrochemical behaviour of the alloy in 0.5M H_2SO_4 solution. The anodic dissolution current density decreases markedly with increasing Mo concentration at the surface but it increases slightly with increasing N concentration. Surface analysis by XPS after passivation shows that N and Mo are segregated on the surface during dissolution and passivation of the alloy. Nitrogen is enriched at the alloy-passive film interface where it may come from nitrides and molybdenum is incorporated in the passive film in the 4^+ and 6^+ chemical states. The passive films formed on the Mo-N impanted alloy have a bilayer structure with an inner oxide layer and outer hydroxide layer. The amount of hydroxide on the passive film seems to be enhanced by the presence of m_o^{6+}.

Introduction

Several studies of the effects of nitrogen and molybdenum on the resistance of stainless steels to general and localized corrosion have been reported (1-14). Ion implantation allows us to obtain high concentrations near the surface of the alloys, which cannot be obtained through classical alloying because of solubility limits, and also to minimize the consumption of alloyed elements needed only for surface interactions. The nitrogen-implanted stainless steel (without Mo) and the molybdenum implanted stainless steel (without N) have already been studied in previous works (15-17) using XPS, RBS and electrochemical measurements. The aim of this